



# Synthesize and Characterization of Pt-supported Co-ZIF for Catalytic Hydrocracking and Hydroisomerization of n-Hexadecane

Luthfiana Nurul Hidayati<sup>1,\*</sup>, Fauzan Aulia<sup>1</sup>, Sebastian Ulido Napitupulu<sup>2</sup>,  
Gede Widia Pratama Adhyaksa<sup>2</sup>, Deliana Dahnum<sup>1,\*</sup>

<sup>1</sup>Research Center for Chemistry, National Research and Innovation Agency, South Tangerang 15314, Indonesia.

<sup>2</sup>Department of Chemical Engineering, Faculty of Industrial Technology, Universitas Pertamina, Jakarta 12220, Indonesia.

Received: 10<sup>th</sup> January 2024; Revised: 22<sup>nd</sup> February 2024; Accepted: 22<sup>nd</sup> February 2024

Available online: 28<sup>th</sup> February 2024; Published regularly: April 2024



## Abstract

Zeolitic Imidazole Frameworks (ZIFs) are prospective porous materials as catalyst support due to their relatively large surface area, and tunability in size, structure, and porosity. Recent studies have also shown that ZIF is the best candidate for various catalytic redox reactions such as the oxidation of benzyl aromatic hydrocarbons. In this study, the synthesized Pt catalyst supported on Co-ZIF was varied by the organic ligands: imidazole, benzimidazole, and 1-(3-aminopropyl) imidazole, then followed by impregnation of Pt precursor. The catalysts were characterized its physical and chemicals properties such as Fourier Transform Infrared (FTIR), X-ray Diffraction (XRD), Scanning Electron Microscope (SEM), and Brunauer Emmet Teller (BET), Temperature-Programmed Desorption (NH<sub>3</sub>-TPD and CO<sub>2</sub>-TPD). The prepared catalysts were evaluated for catalytic hydrocracking and hydroisomerization of n-hexadecane in a 100 ml-batch reactor. GC-MS analysis presented that the Pt/ZIF catalyst with imidazole ligands has better performance than others. Hence, the optimization of n-Hexadecane conversion was carried out by the Pt/ZIF-imidazole catalyst varying the amount of metal loading, time and temperature reaction. The results showed that the reaction temperature of 350 °C using 20 bar H<sub>2</sub> for 4 h and the addition of 15 wt% Pt successfully achieved 90.77% conversion and produced the highest yield of isomers and alkanes, 4.04% and 35.75%, respectively.

Copyright © 2024 by Authors, Published by BCREC Publishing Group. This is an open access article under the CC BY-SA License (<https://creativecommons.org/licenses/by-sa/4.0>).

**Keywords:** Zeolitic Imidazole Frameworks; Metal-Organic Framework; Hydrocracking; Hydroisomerization; n-hexadecane

**How to Cite:** L.N. Hidayati, F. Aulia, S.U. Napitupulu, G.W.P. Adhyaksa, D. Dahnum (2024). Synthesize and Characterization of Pt-supported Co-ZIF for Catalytic Hydrocracking and Hydroisomerization of n-Hexadecane. *Bulletin of Chemical Reaction Engineering & Catalysis*, 19 (1), 171-180 (doi: 10.9767/bcrec.20117)

**Permalink/DOI:** <https://doi.org/10.9767/bcrec.20117>

## 1. Introduction

The study of porous materials is significantly increasing and continues to be studied massively in recent decades. Metal-organic frameworks (MOF) based materials, are porous materials composed of metal precursors and have strong bonds with organic ligands which are often called linkers to compose dimensional materials [1]. MOFs have gained interest because of their excellent properties that have many advantages in used for various purposes. Zeolitic Imidazole Frameworks (ZIFs) are one of the MOF subclasses

which receive outstanding attention. ZIFs are constructed by tetrahedral metal cations M (M=Zn or Co) and imidazolate ligands (Im). The structure consists M-Im-M angle (~145°) which is similar to the Si-O-Si order in prevalent aluminosilicate zeolites, resulting in the zeolite tetrahedral topology also commonly found in most ZIF structures [2,3].

Zeolitic imidazolate frameworks (ZIFs) have several advantages that make them attractive for various applications. Here are some of the advantages of ZIF materials, such as their huge surface area and porosity, thermal and chemical stability making them resistant to thermal changes, and chemical degradation, and suitable

\* Corresponding Author.

Email: luth003@brin.go.id (L.N. Hidayati);  
deli001@brin.go.id (D. Dahnum);

for use in harsh conditions. ZIFs feature a great degree of structural tunability, allowing them to be tailored to specific purposes [4,5]. Hence, the synthesis of ZIF materials is necessary to determine the properties and purposes of the utilized materials. There are diverse procedures for synthesizing ZIFs, including solvothermal or hydrothermal techniques, electrochemical synthesis, and melt-quench method [6,7]. The most widely used technique for synthesizing ZIF-67 is the solvothermal method, where crystals slowly grow from a heated solution of a hydrated metal salt, an ImH (imidazole with an acidic proton), a solvent, and a base. Some also provided ZIF-based materials through hydrothermal/solvothermal synthesis practices in organic solvents. The synthesis of ZIFs requires a combination of metal cations and imidazole linkers which allow for control of ZIF structure [8]. In this study, we applied another method which does not require heating temperature, so this process is more convenient and less harmful. Moreover, it is more environmentally friendly because the solvent used can be recycled and reused. Due to their superior properties especially high porosity and surface area, ZIF materials are used in a wide range of gaseous absorption, semiconductor and electronic devices, biosensors, medicines and drug delivery systems and catalysis applications [9–13].

ZIFs and their derivatives have shown great potential as heterogeneous catalysts for various chemical reactions including acid-base catalysis, size-selective catalysis, and electrocatalysis [6,14]. Their unique structure and properties contribute to their enhanced catalytic performance. They also easily can be reusable and combined with other materials such as polymers, carbon-based materials, or other metal precursors to enhance their catalytic properties or facilitate their application in specific systems [15]. Their unique structure and properties contribute to their enhanced catalytic performance. In addition, modification by changing metal cations and various organic linkers can modulate the morphology and size of ZIF crystals thereby affecting the functional properties of the material. The combination of suitable metal and organic linkers makes the designed ZIF have numerous tunable properties with different molecular sizes, structures, as well as pore sizes [8]. Cobalt-Imidazole frameworks, composed of  $\text{Co}^{2+}$  metals and imidazole linkers, were proved to have the ability as precursors for Oxygen Reduction Reactions [16]. As reported, Cobalt-Imidazole has 305  $\text{m}^2/\text{g}$  of BET surface area and 0.8-1.3 nm of pore size. In addition, when the imidazole was changed to benzimidazole, the surface area and the pore size were found differently. Ren et.al reported Cobalt-Benzimidazole had a BET surface

area of 75.3337  $\text{m}^2/\text{g}$  with 3.88 nm of pore size [17]. Indeed, the selection of organic linkers affected the properties of ZIF materials. Our previous study, ZIF-67 which is constructed of cobalt metals and 2-methylimidazole linkers had a BET surface of 892.74  $\text{m}^2/\text{g}$  and pore size 15-100 nm. The ZIF-67 loaded with Pt-nps showed catalytic activity in the hydrocracking and hydroisomerization of long-chain alkanes [18].

Hydroisomerization of long-chain alkanes is a process that is used to lower the pour point and to obtain a high viscosity index, which enhances the cold flow properties of fuels without reducing the cetane number. The process involves converting straight-chain alkanes into branched isomers, which have lower melting points and improve cold flow properties making them more favorable for usage in low-temperature environments [19,20]. According to many studies, the selective catalyst greatly determines the transformation of straight-chain alkanes into branched chains by reducing the occurrence of cracking. The hydroisomerization reaction takes place on bifunctional catalysts consisting of both metal sites for hydrogenation/dehydrogenation and Brønsted acid sites for isomerization [20]. The iso/normal ratio increases significantly with carbon number, suggesting that isomerization of higher alkanes occurs before cracking. The influence of carbon chain length of alkanes on hydrogen isomerization was investigated and it was found that the conversion of n-alkanes decreased with increasing chain length [21]. Hydroisomerization can produce high-quality hydrocarbon products that meet the requirements for a variety of applications.

Hydrocarbon isomerization has been intensively investigated for decades, although it remains unclear which specific catalysts and methods can produce high isomer yields. Mesoporous acid catalysts, especially aluminosilicates and zeolites, tend to crack into short-chain hydrocarbons rather than isomers. Our previous study revealed using Pt/ZIF-67 catalyst, a long chain hydrocarbon of hexadecane was converted to  $\text{nC}_8\text{-C}_{15}$  of alkane and  $\text{iC}_8\text{-C}_{15}$  of iso-alkane yields of 21.38% and 2.45%, respectively [18].

In this study, we developed cobalt-ZIF materials loaded with Pt nanoparticles (nps) and evaluated their catalytic activity in hydrocracking and hydroisomerization reactions of long-chain alkanes. Co-ZIF materials were synthesized by the modification of the ZIF structure ZIF through changes in various organic ligands, including imidazole, benzimidazole, and 1-(3-aminopropyl) imidazole. The different ligands could be used as a structure-directing agent so that the surface area and pore size were tunable by the length of the linker. Imidazole ligand is the basic form of

imidazole organic linker, while benzimidazole is composed of a benzene ring fused with an imidazole ring. The 1-(3-aminopropyl) imidazole was selected as an organic linker because of the addition of amino groups attached to the imidazole ring. Different linkers used on cobalt-ZIF might affect the acidity of properties which play an important role in the catalytic process. The synthesized Co-ZIF was loaded with Pt nanoparticles (nps) in which Pt was suggested to be a promising active catalyst metal to carry out hydroisomerization reactions. For the reactant, hexadecane was chosen as a model compound due to it represents a long-chain carbon that was difficult to form isomers. Here, we investigated the effect of different imidazole linkers of Co-ZIF loaded Pt-nps and its effectiveness as a catalyst for hydrocracking and hydroisomerization of hexadecane.

## 2. Materials and Methods

### 2.1 Chemical Materials

The chemicals were purchased commercially and directly used without any further purification process. Imidazole, Benzimidazole, 1-(3-aminopropyl) imidazole, Chloroplatinic acid hexahydrate  $\text{H}_2\text{PtCl}_6 \cdot 6\text{H}_2\text{O}$  ( $\geq 99.9\%$  Pt basis), and n-Hexadecane 99% were purchased from Sigma-Aldrich. Cobalt(II) nitrate hexahydrate ( $\text{Co}(\text{NO}_3)_2 \cdot 6\text{H}_2\text{O}$ ), Diethylamine (DEA), Methanol ( $\text{MeOH}$ ), and Dichloromethane (DCM) as a solvent for GC-MS analysis were obtained from Merck.

### 2.2 Catalyst Preparation

The ZIF-catalysts were synthesized following this method [18] by adding  $\text{Co}(\text{NO}_3)_2 \cdot 6\text{H}_2\text{O}$  and imidazole with a mass ratio of 1 : 2, into 150 mL of methanol. Then, 25 mL of diethyl amine was added to the mixture and stirred constantly at room temperature for 48h. The precipitated solid in the solution was collected by centrifuge at 5000 rpm for 5 min then was dried at 130 °C for 3 h by vacuum oven to evaporate the methanol remained. The formed solid was calcined at 250 °C for 3 h to remove the impurities for further utilization. The material was referred to as ZIF-Imidazole. A similar procedure was repeated by replacing Imidazole with Benzimidazole and 1-(3-aminopropyl) imidazole, then denoted as ZIF-Benzimidazole and ZIF-1-(3-aminopropyl) imidazole, respectively.

Pt/ZIF-imidazole catalyst was prepared by wet impregnation method. An amount of 15 wt% Pt metal was added to ZIF-imidazole. Chloroplatinic acid hexahydrate as Pt source and ZIF-imidazole were added to 150 mL of methanol in a round flask. The mixture was stirred under

reflux at 60 °C for 24 h. The solid was collected by using a rotary vacuum evaporator, then it was dried at 130 °C for 3 h in the vacuum oven. The obtained Pt/ZIF-imidazole catalyst was calcined at 250 °C for 3 h and reduced under  $\text{H}_2$  gas flow at 300 °C for 3 h. Similar procedures were repeated for using ZIF-Benzimidazole and ZIF-1-(3-aminopropyl) imidazole. The obtained solid was denoted as Pt/ZIF-benzimidazole and Pt/ZIF-1-(3-aminopropyl) imidazole, respectively.

### 2.3 Catalysts Characterization

$\text{N}_2$  physisorption was conducted by Brunauer-Emmett Teller (BET) Micromeritics TriStar II 3020 to analyze the surface area and porosity of synthesized catalysts. The X-ray diffraction (XRD) pattern of catalyst crystallinity was obtained by XRD Rigaku Smart Lab Cu-K $\alpha$  with the  $2\theta$  angle between 5° to 80°. The infrared spectra (FT-IR) were recorded by Shimadzu IR Prestige-21 to analyze the functional organic group contained in the catalyst material structure. Field Emission-Scanning Electron Microscope (FE-SEM) JIB-4610F was used to observe the morphology of catalysts. Chemisorption analysis including Temperature-Programmed Desorption of Ammonia ( $\text{NH}_3$ -TPD) Micromeritics ChemiSorb 2750 to analyze and quantify the acidity properties of the catalysts. The sample's pretreatment was degassed at 200 °C, then the desorption was at 400 °C and held for 30 min.

### 2.4 Catalytic Performance Test

The catalytic hydrocracking and hydroisomerization reactions were conducted in a high-pressure batch autoclave reactor. In this study, N-hexadecane was used as a model compound of long-chain hydrocarbons. The catalyst loading was set at 10 wt% of the reactant and placed in the reactor chamber. The  $\text{H}_2$  gas was purged before the reaction. The hydrogenation was carried out at varied temperatures of 300-370 °C, and 20 bar of  $\text{H}_2$ , and reaction time was varied from 2-8 h. The liquid products were collected and analyzed by Gas Chromatography-Mass Spectrometry (GC-MS) (Agilent 7890A) with an HP-5 capillary column (30m  $\times$  0.25mm  $\times$  0.25  $\mu\text{m}$ ).

The quantification of the results including the conversion of hexadecane, yields of products including n-alkane ( $\text{nC}_9$ - $\text{C}_{15}$ ), and isomer ( $\text{iC}_8$ - $\text{C}_{15}$ ) were calculated based on the reported paper [22].

$$AC = \frac{\text{Total peak area} - \text{Peak area of nC16}}{\text{Total peak area}} \times 100\% \quad (1)$$

$$\text{Hexadecane conversion} = \frac{\text{weight of RM} - \text{weight of LP} + (\text{weight of LP} \times AC)}{\text{weight of RM}} \times 100\% \quad (2)$$

Yield of products =

$$\frac{\text{peak area of } n\text{C8-C15 or } i\text{C8-C15}}{\text{total peak area}} \times \frac{\text{weight of LP}}{\text{weight of RM}} \times 100\% \quad (3)$$

wherein, AC = apparent conversion; LP = liquid product; RM = raw material. Meanwhile, the percentage product distribution of each product was calculated using:

%Product =

$$\frac{\text{Area of each product obtained by GCMS}}{\text{Area of total product obtained by GCMS}} \times 100\% \quad (4)$$

### 3. Results and Discussion

#### 3.1 X-Ray Diffraction (XRD) Analysis

The XRD determines the crystal structures which are formed from the synthesis of Pt-supported ZIFs catalysts. Figure 1 shows the XRD pattern of ZIF-Imidazole and Pt/ZIF-Imidazole. ZIF-Imidazole shows the main peaks located at  $2\theta$  values of  $15.13^\circ$ ,  $17.13^\circ$ ,  $18.62^\circ$ , and  $20.85^\circ$ . The sharp diffraction peaks obtained can be related to the highly crystalline structure of the ZIF-

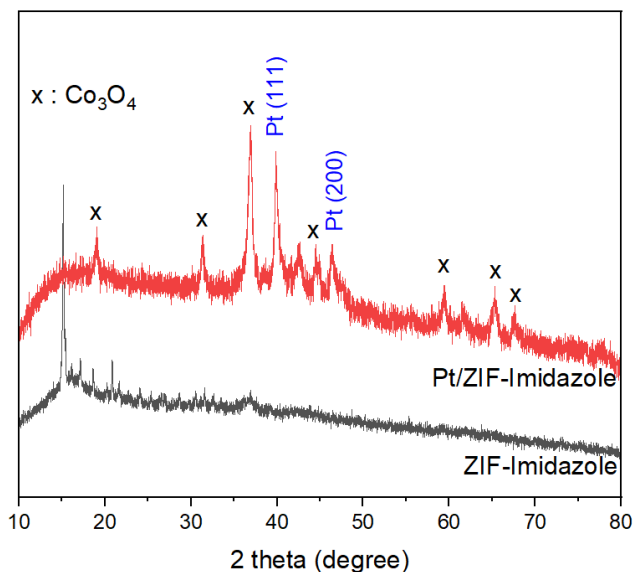


Figure 1. XRD pattern of ZIF-Imidazole and Pt/ZIF-Imidazole.

Imidazole. In Figure 1 the XRD pattern of ZIF-Imidazole and Pt/ZIF-Imidazole have quite a lot of differences, which means that Pt addition to the ZIF-Imidazole catalyst causes decomposition of the ZIF-Imidazole form and changed the trend. The heat treatment temperature affected the intensity and sharpness of the Pt peaks due to increased crystallinity and dispersion of Pt on the ZIF-imidazole surface which could raise the density of the metal active sites. It is also indicated that a derivative of ZIF-Imidazole, detected as cobalt oxide ( $\text{Co}_3\text{O}_4$ ) formed after the addition of Pt and was exposed to heat treatment such as calcination and  $\text{H}_2$  reduction. Herein, the other peaks observed in the ZIF-imidazole are consistent with  $hkl$  of (220), (311), (511), and (440) as  $\text{Co}_3\text{O}_4$  which showed at the sharp diffraction peaks at  $2\theta = 31.35^\circ$ ,  $36.91^\circ$ ,  $59.35^\circ$ , and  $65.34^\circ$ . The XRD pattern of Pt/ZIF-imidazole showed the high intensity of Pt peak at  $2\theta$  of  $39.86^\circ$  and  $46.33^\circ$ , assigned to the Pt(111) and Pt(200).

#### 3.2 Surface Area and Porosity Analysis

The surface area and porosity of the synthesized Pt/Co-ZIF with various organic ligands after calcined and reduced were analyzed by Brunauer Emmet Teller (BET) and Barrett-Joyner-Halenda (BJH). The sorption isotherms and pore size distribution of synthesized catalysts are shown in Figure 2. Table 1 presents the  $\text{N}_2$  physisorption analysis. The ZIF-Imidazole catalyst showed a surface area of  $33.81 \text{ m}^2/\text{g}$  which then decreased to  $6.82 \text{ m}^2/\text{g}$  after Pt metal was impregnated. This is probably because the ZIF-Imidazole pores are blocked by Pt metal particles. The pore volume also decreased from  $0.099 \text{ cm}^3/\text{g}$  to  $0.018 \text{ cm}^3/\text{g}$  after Pt addition, indicating that the Pt metal occupied the pores on the surface of the ZIF-Imidazole catalyst. ZIF-Benzimidazole has a relatively similar trend as ZIF-Imidazole, wherein the surface area and pore volume decrease after Pt loading. On the other hand, the ZIF-1-(3-Aminopropyl) imidazole showed the surface area and pore volume increased considerably from  $4.78 \text{ m}^2/\text{g}$  to  $17.99 \text{ m}^2/\text{g}$  after Pt addition. It might be because the distribution of Pt particles does not completely cover the pores.

Table 1. Physical properties of the synthesized catalyst.

| Synthesized catalyst               | BET Surface Area ( $\text{m}^2/\text{g}$ ) | Micropore Surface Area ( $\text{m}^2/\text{g}$ ) | Pore volume ( $\text{cm}^3/\text{g}$ ) | Pore size (nm) |
|------------------------------------|--|--|--|----------------|
| ZIF-Imidazole                      | 33.81                                      | 6.89   | 0.099                                  | <2, 15–100     |
| Pt/ZIF-Imidazole                   | 6.82                                       | 11.12  | 0.018                                  | 20-100         |
| ZIF-Benzimidazole                  | 31.22                                      | nd   | 0.084                                  | <2, 12-100     |
| Pt/ZIF-Benzimidazole               | 3.58                                       | 0.45   | 0.010                                  | 12-100         |
| ZIF-1-(3-Aminopropyl)imidazole)    | 4.78                                       | 1.08   | 0.018                                  | <2, 15–100     |
| Pt/ZIF-1-(3-Aminopropyl)imidazole) | 17.99                                      | 2.82   | 0.038                                  | <5, 15-100     |

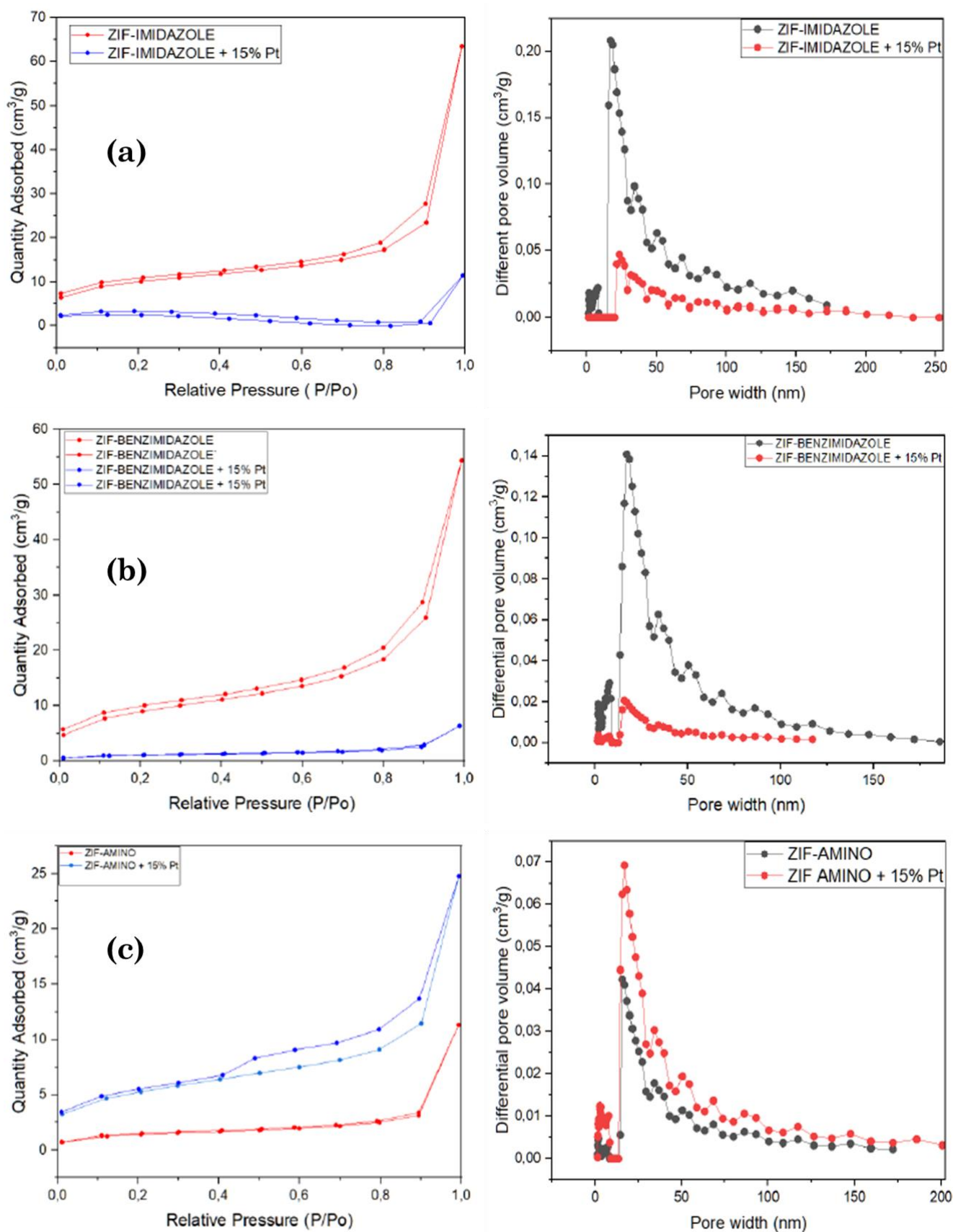


Figure 2. The sorption isotherms and the pore size distribution of (a) Pt/ZIF-Imidazole; (b) Pt/ZIF-Benzimidazole; (c) Pt/ ZIF-1-(3-Aminopropyl) imidazole.



### 3.3 Fourier Transform Infrared Spectroscopy

Furthermore, the FT-IR spectra of the catalysts are presented in Figure 3. The FTIR spectra of ZIF materials with 3 different ligands such as imidazole, benzimidazole and 1-(3-Aminopropyl) imidazole showed some similarities with ZIF-67 [18]. It can be seen from Figure 3(a) that in Pt/ZIF-Imidazole, the changes are quite different from ZIF-Imidazole before impregnated with Pt. It is probably because the Pt metal has not been completely immersed into the ZIF-

Imidazole catalyst. The bands at 693 and 753  $\text{cm}^{-1}$  are out-of-plane bending, whereas the peaks in the region of between 900 and 1350  $\text{cm}^{-1}$  refer to the imidazole ring [22]. As for ZIF-Imidazole, the absorption bands at 754  $\text{cm}^{-1}$  refer to with out-of-plane bending of the imidazole ring, while the one appearing at 1500  $\text{cm}^{-1}$  is associated with the stretching vibration of the entire imidazole ring [23]. Different spectra in Figure 3(b) exhibit the benzimidazole ligands. The addition of Pt shows almost similar behaviour to the peaks of the

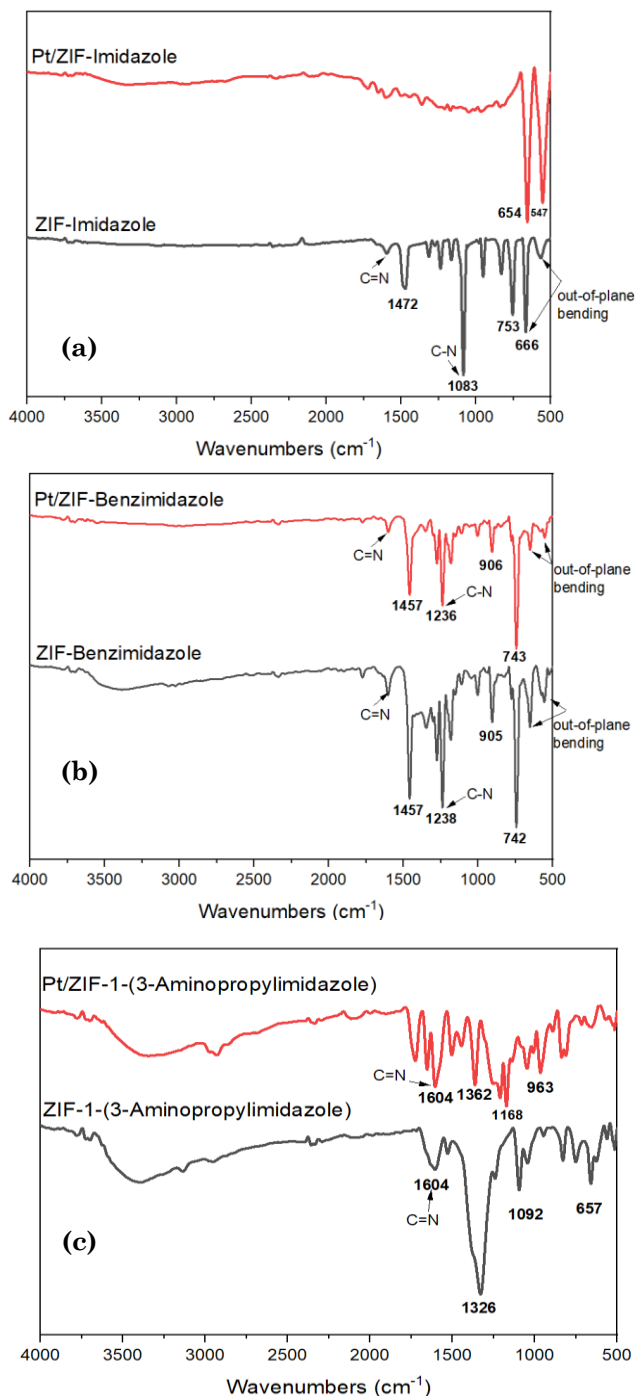


Figure 3. FT-IR spectra of (a) Pt/ZIF-Imidazole; (b) Pt/ZIF-Benzimidazole; (c) Pt/ ZIF-1-(3-Aminopropyl) imidazole.

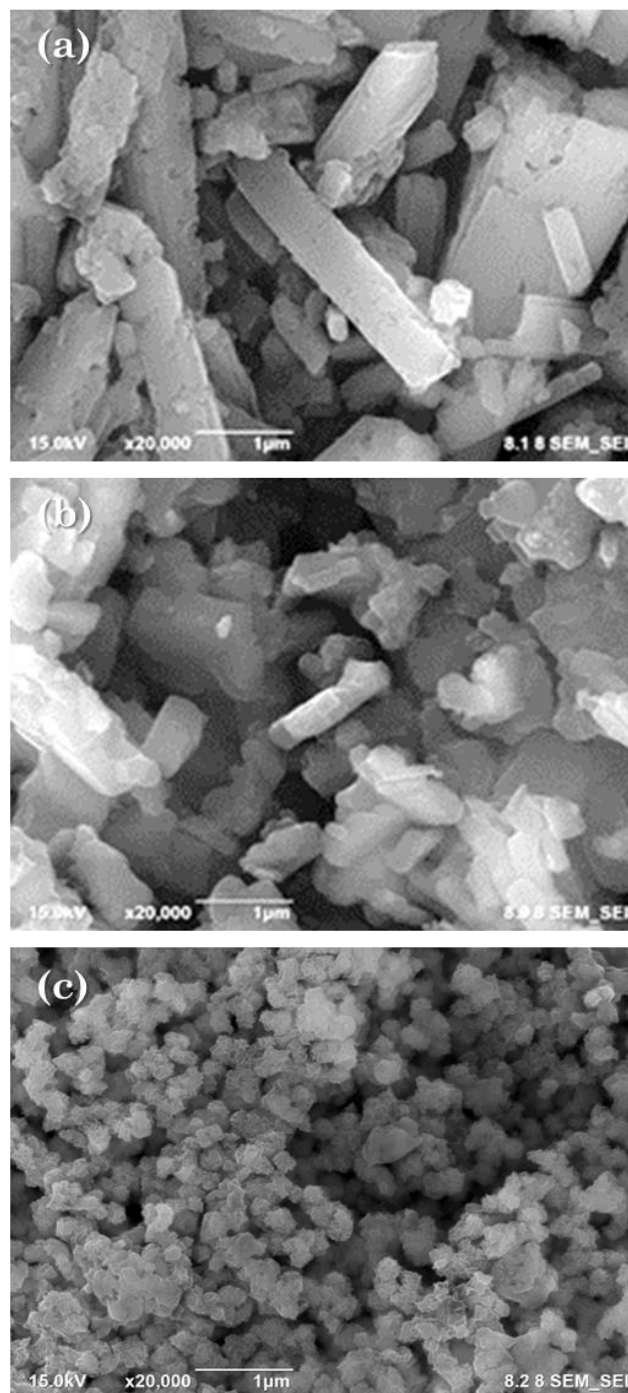


Figure 4. SEM analysis of (a) ZIF-Imidazole, (b) ZIF-Benzimidazole, (c) ZIF-1-(3-Aminopropyl) imidazole.

spectrum in the FTIR spectra. It indicates that Pt is completely absorbed by the catalyst component which shows relatively the same stretching bond. The spectra are also shown at the peak of  $1083\text{ cm}^{-1}$  indicating the formation of C-N. The ZIF catalyst using the 1-(3-aminopropyl) imidazole ligand in Figure 3(c) shows the imidazole ring formed as well, although it has lower intensity compared to the previous ligand, this is shown at peaks of  $1168\text{ cm}^{-1}$ ,  $1362\text{ cm}^{-1}$ , and  $1604\text{ cm}^{-1}$  retained on the catalyst structure [22].

### 3.4 Scanning Electron Microscope

Scanning Electron Microscope (SEM) analysis to observe the surface morphological structure of the ZIFs catalysts and also to find out the elements and crystals which are formed from synthesized catalysts. SEM figures (Figure 4) describe different shapes and morphology depending on the organic ligands which are applied. In the ZIF-Imidazole catalyst, it is known that the resulting form is in the form of a long rod, while in the ZIF-Benzimidazole and ZIF-1-(3-aminopropyl) imidazole catalysts it slightly resembles a rhombic dodecahedral shape or a shape resembles a cube.

### 3.5 Ammonia Temperature-Programmed Desorption (NH<sub>3</sub>-TPD)

Temperature-Programmed Desorption (NH<sub>3</sub>-TPD) was conducted to measure the acidity properties of the catalysts which play the key role in the hydroisomerization of long-chain alkanes. The acidity profile is classified into 3 regions: weak acid in the temperature range  $100\text{--}250\text{ }^{\circ}\text{C}$ , medium acid in  $250\text{--}400\text{ }^{\circ}\text{C}$ , and strong acid in  $>400\text{ }^{\circ}\text{C}$  [24]. Figure 5 exhibits the profile that

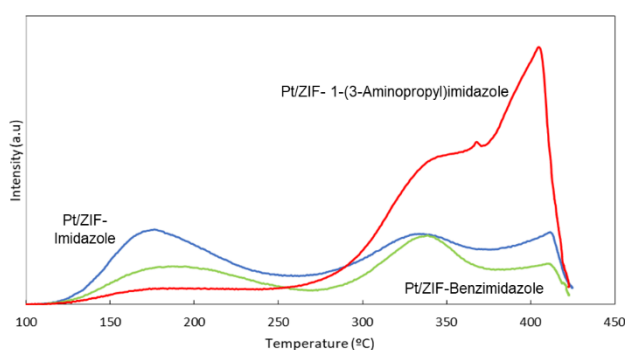


Figure 5. NH<sub>3</sub>-TPD profile of the catalysts.

illustrates the Pt/Imidazole catalyst has a similar trend to the Pt/Benzimidazole catalyst. The weak acid was detected at a peak of  $160\text{ }^{\circ}\text{C}$ , medium acid at a peak of  $370\text{ }^{\circ}\text{C}$ , and strong acid at  $422\text{ }^{\circ}\text{C}$ . The peak intensity of the Pt/ZIF-Imidazole catalyst is slightly higher than Pt/ZIF-Benzimidazole. It corresponds to the number of acidity moles of Pt/ZIF-Imidazole being greater as shown in Table 2. Whereas in Pt/ZIF-1-(3-aminopropyl) imidazole shows only strong acids with very high intensity, while weak and medium acids are slightly detected.

Table 2 represents the quantification of the NH<sub>3</sub>-TPD profile in Figure 5. Pt/ZIF-Imidazole has higher acidity than Pt/Benzimidazole. While, Pt/ZIF-1-(3-aminopropyl) imidazole has two times higher number of acidity moles than others. Catalysts with shape-selective properties, such as zeolites, can exhibit enhanced selectivity towards isomerization due to their specific pore structures and acid distributions. The distribution and amount of metal on the catalyst surface can interact with the acidity and influence the selectivity of the hydroisomerization reaction [19].

### 3.6 Catalytic Performance Test

The hydroisomerization of n-hexadecane was carried out in a 100 mL batch reactor pressured with H<sub>2</sub> gas. The catalysts loading was 10wt% of n-Hexadecane without solvent added. The liquid product was analyzed by GC-MS to determine the chemical compounds. The product distribution (Figure 6) shows that Pt/ZIF-Imidazole has better performance than other catalysts. It resulted in both the isomers compound and cracking products of n-hexadecane. Even though the Pt/Benzimidazole catalyst is selective toward isomer products only, its conversion is also very limited. Whilst the Pt/ZIF-1-(3-aminopropyl) imidazole catalyst resulted in the least isomer products. This mechanism involves the cooperation of both acid and metal sites on the catalyst surface. The alkane molecule is first adsorbed onto the acid site, where the isomerization has occurred to form a carbocation intermediate. The carbocation then migrates to the metal site, where it undergoes hydrogenation to form a branched-chain isomer [23].

The acidity of the catalyst plays a crucial role in the selectivity of the hydroisomerization of long-chain paraffins. The strength of the acid sites on the catalyst surface can influence the

Table 2. The catalysts' acidity quantification.

| Catalyst                           | Acidity (mmol/g) |
|------------------------------------|------------------|
| Pt/ZIF-Imidazole                   | 1.882            |
| Pt/Benzimidazole                   | 1.212            |
| Pt/ZIF-1-(3-aminopropyl) imidazole | 2.905            |

selectivity towards isomerization or cracking reactions [25,26]. Stronger acid sites are more likely to promote cracking, while weaker acid sites aim for isomerization. This is correlated with the  $\text{NH}_3$ -TPD profile in Figure 5 wherein Pt/ZIF-Imidazole has 3 strength acidity components (weak, medium, and strong) with intensity higher than Pt/Benzimidazole. While Pt/ZIF-1-(3-aminopropyl) imidazole majority consists of strong acidity which is not favourable for isomerization reaction. According to the results above, the reaction condition optimization is going to use the Pt/ZIF-Imidazole catalyst.

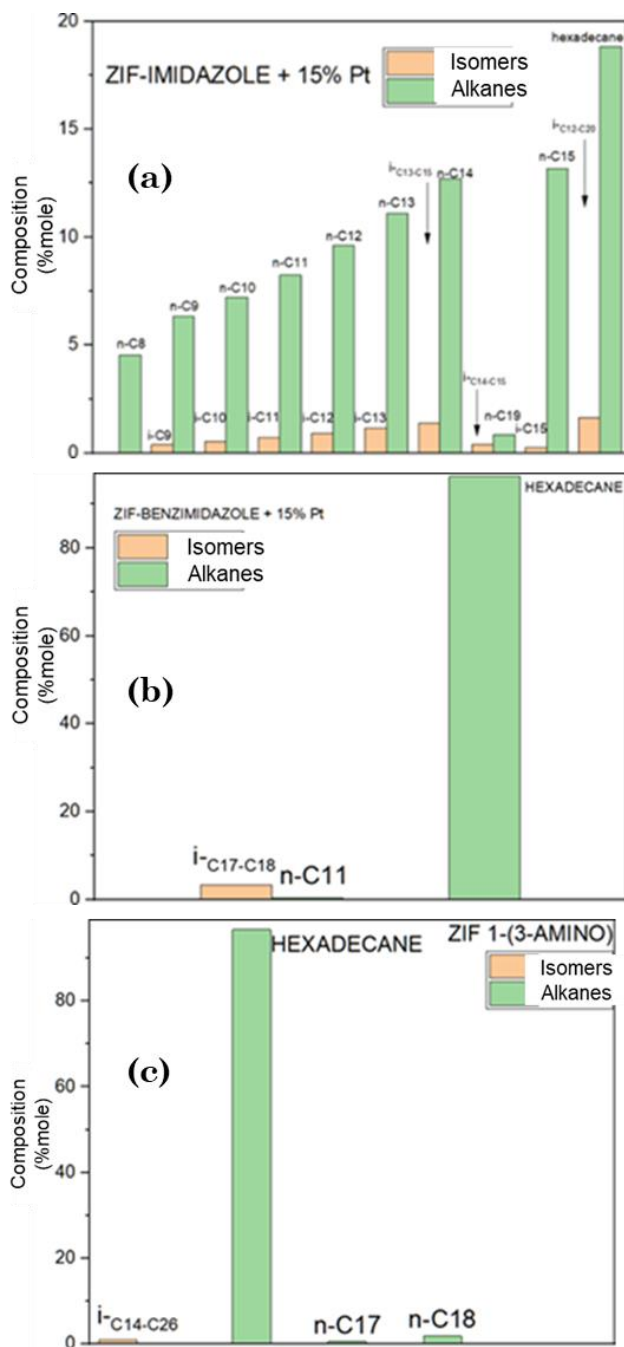


Figure 6. Products distribution of catalysts with various organic ligands: (a) Pt/ZIF-Imidazole; (b) Pt/Benzimidazole; (c) Pt/ZIF-1-(3-aminopropyl) imidazole.

The loading of Pt metal was varied from 5 wt%, 10 wt% and 15 wt%. The highest yield is produced by impregnating 15 wt% of Pt into ZIF-Imidazole with resulting isomers and alkanes yield of 35.75% and 4.04%, respectively. The 15 wt% Pt/ZIF-Imidazole was chosen as the catalyst to carry out the optimization of reaction temperature and time.

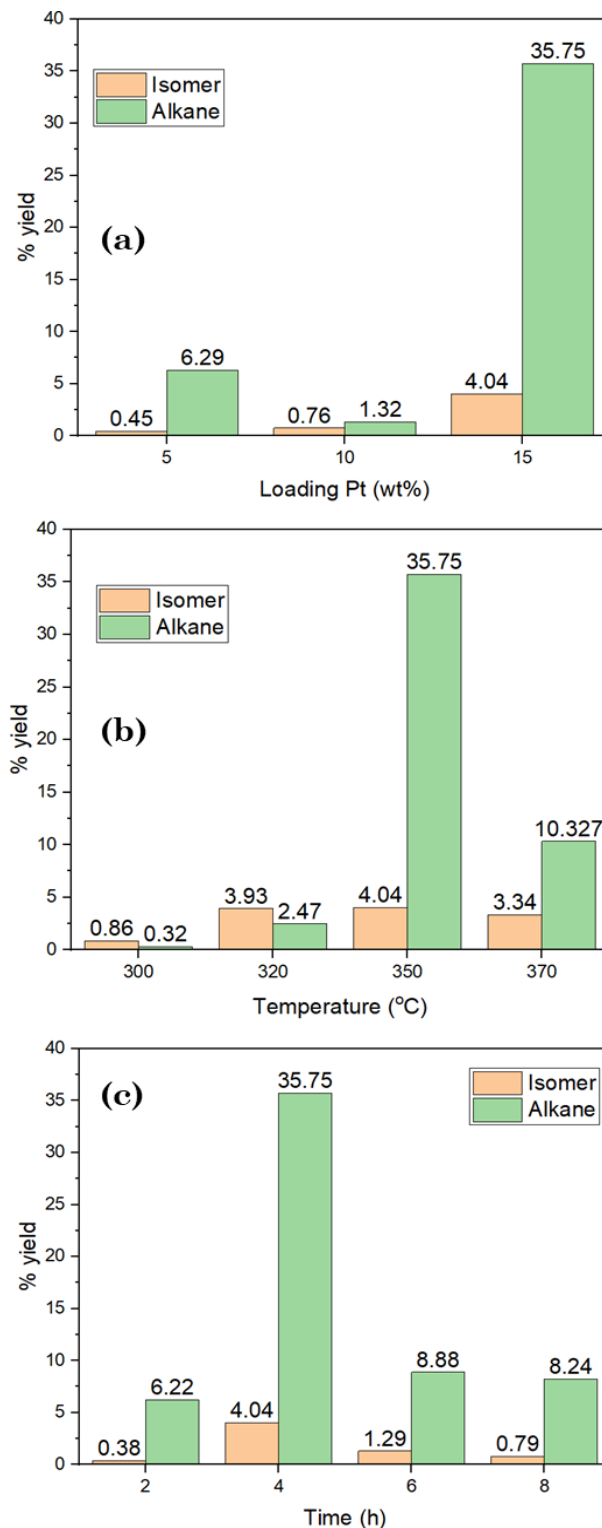


Figure 7. Optimization of reaction condition of hydroisomerization of n-Hexadecane: (a) Effect of loading Pt metal on ZIF-Imidazole; (b) Effect of reaction temperature; (c) effect of reaction time.



Increasing temperatures from 300 °C, 320 °C, to 350 °C shows a rise in the yield of isomer and alkane products. Whereas when the temperature was increased up to 370 °C, the product yield plummeted drastically. A temperature of 350 °C is considered as optimal temperature for isomerization reactions using a 15 wt% Pt/ZIF-Imidazole catalyst. In Figure 7(c) can be seen that the reaction time that produces the highest yield is 4h then the yield is decreased along with the longer reaction time and it does not show any significant results.

The liquid products of hydrogenation of n-hexadecane over 15 wt% Pt/ZIF-Imidazole catalyst under optimized conditions: 350 °C, 4h, 20 bar H<sub>2</sub> was analyzed by GC-MS to determine the chemical compounds products. The conversion of n-hexadecane was obtained at 90.77%, which means the catalyst performs well in converting the reactants into hydrocarbon cracking and isomer derivatives products of n-hexadecane. They are summarized as follows nC<sub>9</sub>-C<sub>15</sub> compounds: nonane, decane, undecane, dodecane, tridecane tetradecane, and Pentadecane. Meanwhile the isomers products, such as iC<sub>8</sub>-C<sub>15</sub>: 2-methyl-octane, 2-methyl-nonane, 2-methyl-decane, 2-methyl-undecane, 2-methyl-dodecane, 2-methyl-tridecane, 2-methyl-eicosane, and 2-methyl-nonadecane.

#### 4. Conclusions

Pt-derived ZIF-catalyst has been successfully synthesized with various types of organic ligands such as imidazole, benzimidazole and 1-(3-aminopropyl) imidazole. It was found that different ligands affect the physical and chemical properties such as morphological shape, surface area, and acidity. ZIF-Imidazole was deformed into cobalt oxide (Co<sub>3</sub>O<sub>4</sub>) which was formed after the addition of Pt and was exposed to heat treatment such as calcination and H<sub>2</sub> reduction. The catalyst that produced a high conversion of n-hexadecane was Pt/ZIF-Imidazole with 15 wt% loading of Pt metal under optimum conditions of 350 °C, 20 bar of H<sub>2</sub> gas, for 4 h. The alkanes and isomers yields were 35.75% and 4.04%, respectively.

#### Acknowledgment

This work was financially funded by Research organization of Nanotechnology and Materials, National Research and Innovation Agency of Republic Indonesia (ORNM-BRIN) FY 2022. We also declared that there is no conflict of interest in this publication.

#### CRedit Author Statement

Authors Contributions: *L. N. Hidayati*: Conceptualization, Methodology, Visualization, Writing, Review and Editing. *F. Aulia*: Formal Analysis, Project Administration. *S. U. Napitupulu*: Investigation, Writing Draft Preparation. *G.W.P. Adhyaksa*: Validation, Formal Analysis. *D. Dahnum*: Conceptualization, Investigation, Methodology, Resources, Supervision. All authors have read and agreed to the published version of the manuscript.

#### References

- [1] Yaghi, O.M., Li, H. (1995). Hydrothermal Synthesis of a Metal-Organic Framework Containing Large Rectangular Channels. *Journal of the American Chemical Society*, 117(41), 10401–10402. DOI: 10.1021/ja00146a033.
- [2] Ding, M., Flaig, R.W., Jiang, H.-L., Yaghi, O.M. (2019). Carbon capture and conversion using metal-organic frameworks and MOF-based materials. *Chemical Society Reviews*, 48(10), 2783–2828. DOI: 10.1039/C8CS00829A.
- [3] Zhong, G., Liu, D., Zhang, J. (2018). The application of ZIF-67 and its derivatives: adsorption, separation, electrochemistry and catalysts. *Journal of Materials Chemistry A*, 6(5), 1887–1899. DOI: 10.1039/C7TA08268A.
- [4] Chen, B., Yang, Z., Zhu, Y., Xia, Y. (2014). Zeolitic imidazolate framework materials: recent progress in synthesis and applications. *Journal of Materials Chemistry A*, 2(40), 16811–16831. DOI: 10.1039/C4TA02984D.
- [5] Wang, H., He, Q., Liang, S., Li, Y., Zhao, X., Mao, L., Zhan, F., Chen, L. (2021). Advances and perspectives of ZIFs-based materials for electrochemical energy storage: Design of synthesis and crystal structure, evolution of mechanisms and electrochemical performance. *Energy Storage Materials*, 43, 531–578. DOI: DOI: 10.1016/j.ensm.2021.09.023.
- [6] Duan, C., Yu, Y., Hu, H. (2022). Recent progress on synthesis of ZIF-67-based materials and their application to heterogeneous catalysis. *Green Energy & Environment*, 7(1), 3–15. DOI: DOI: 10.1016/j.gee.2020.12.023.
- [7] Shahsavari, M., Mohammadzadeh Jahani, P., Sheikhsheae, I., Tajik, S., Aghaei Afshar, A., Askari, M.B., Salarizadeh, P., Di Bartolomeo, A., Beitollahi, H. (2022). Green Synthesis of Zeolitic Imidazolate Frameworks: A Review of Their Characterization and Industrial and Medical Applications. *Materials*, 15(2), 447. DOI: 10.3390/ma15020447.
- [8] Zhang, H., Duan, C., Li, F., Yan, X., Xi, H. (2018). Green and rapid synthesis of hierarchical porous zeolitic imidazolate frameworks for enhanced CO<sub>2</sub> capture. *Inorganica Chimica Acta*, 482, 358–363. DOI: 10.1016/j.ica.2018.06.034.

- [9] Meshkat, S., Kaliaguine, S., Rodrigue, D. (2020). Comparison between ZIF-67 and ZIF-8 in Pebax®MH-1657 mixed matrix membranes for CO<sub>2</sub> separation. *Separation and Purification Technology*, 235, 116150. DOI: 10.1016/j.seppur.2019.116150.
- [10] Qian, J., Sun, F., Qin, L. (2012). Hydrothermal synthesis of zeolitic imidazolate framework-67 (ZIF-67) nanocrystals. *Materials Letters*, 82, 220–223. DOI: 10.1016/j.matlet.2012.05.077.
- [11] Burtch, N.C., Jasuja, H., Walton, K.S. (2014). Water Stability and Adsorption in Metal–Organic Frameworks. *Chemical Reviews*, 114(20), 10575–10612. DOI: 10.1021/cr5002589.
- [12] Wang, Q., Sun, Y., Li, S., Zhang, P., Yao, Q. (2020). Synthesis and modification of ZIF-8 and its application in drug delivery and tumor therapy. *RSC Advances*, 10 (62), 37600–37620. DOI: 10.1039/D0RA07950B.
- [13] Yu, Y., Yin, Q.-G., Ye, L.-J., Yu, H. (2023). Retraction Note: Porous Zn(II)-organic framework with tetrazolyl decorated pores for selective C<sub>2</sub>H<sub>2</sub> adsorption and treatment activity on infantile meningitis. *Macromolecular Research*, 31 (6), 635. DOI: 10.1007/s13233-023-00153-6.
- [14] Khrizanforov, M. (2023). Editorial of Special Issue Synthesis and Molecular Applications of Metal-Organic Frameworks (MOFs; *International Journal of Molecular Sciences*, 24(9), 7857. DOI: 10.3390/ijms24097857.
- [15] Pouramini, Z., Mousavi, S.M., Babapoor, A., Hashemi, S.A., Lai, C.W., Mazaheri, Y., Chiang, W.-H. (2023). Effect of Metal Atom in Zeolitic Imidazolate Frameworks (ZIF-8 & 67) for Removal of Dyes and Antibiotics from Wastewater: A Review. *Catalysts*, 13 (1), 155. DOI: 10.3390/catal13010155.
- [16] Ma, S., Goenaga, G.A., Call, A. V, Liu, D.-J. (2011). Cobalt imidazolate framework as precursor for oxygen reduction reaction electrocatalysts. *Chemistry*, 17 (7), 2063–2067. DOI: 10.1002/chem.201003080.
- [17] Ren, W., Gao, J., Lei, C., Xie, Y., Cai, Y., Ni, Q., Yao, J. (2018). Recyclable metal-organic framework/cellulose aerogels for activating peroxymonosulfate to degrade organic pollutants. *Chemical Engineering Journal*, 349, 766–774. DOI: 10.1016/j.cej.2018.05.143.
- [18] Ramadhita, H., Aulia, F., Hidayati, L.N., Bakti, A.N., Simanjuntak, F.S.H., Dahnum, D. (2023). Pt/ZIF-67-derived PtxCo<sub>3</sub>O<sub>4</sub> catalyst for hydrocracking and hydro-isomerization of n-hexadecane. *AIP Conference Proceedings*, 2902(1), 30016. DOI: 10.1063/5.0172851.
- [19] Mäki-Arvela, P., Kaka khel, T.A., Azkaar, M., Engblom, S., Murzin, D.Y. (2018). Catalytic Hydroisomerization of Long-Chain Hydrocarbons for the Production of Fuels. *Catalysts*, 8 (11), 534. DOI: 10.3390/catal8110534.
- [20] Jaroszevska, K., Masalska, A., Grzechowiak, J.R. (2020). Hydroisomerization of long-chain bio-derived n-alkanes into monobranched high cetane isomers via a dual-component catalyst bed. *Fuel*, 268, 117239. DOI: 10.1016/j.fuel.2020.117239.
- [21] Calemma, V., Peratello, S., Perego, C. (2000). Hydroisomerization and hydrocracking of long chain n-alkanes on Pt/amorphous SiO<sub>2</sub>–Al<sub>2</sub>O<sub>3</sub> catalyst. *Applied Catalysis A: General*, 190 (1), 207–218. DOI: 10.1016/S0926-860X(99)00292-6.
- [22] Ammar, M., Jiang, S., Ji, S. (2016). Heteropoly acid encapsulated into zeolite imidazolate framework (ZIF-67) cage as an efficient heterogeneous catalyst for Friedel–Crafts acylation. *Journal of Solid State Chemistry*, 233, 303–310. DOI: 10.1016/j.jssc.2015.11.014.
- [23] Al-Fakih, A., Ahmed Al-Koshab, M.Q., Al-Awsh, W., Drmash, Q.A., Al-Osta, M.A., Al-Shugaa, M.A., Onaizi, S.A. (2022). Mechanical, hydration, and microstructural behavior of cement paste incorporating Zeolitic imidazolate Framework-67 (ZIF-67) nanoparticles. *Construction and Building Materials*, 348, 128675. DOI: 10.1016/j.conbuildmat.2022.128675.
- [24] Pimerzin, A., Savinov, A., Vutolkina, A., Makova, A., Glotov, A., Vinokurov, V., Pimerzin, A. (2020). Transition Metal Sulfides- and Noble Metal-Based Catalysts for N-Hexadecane Hydroisomerization: A Study of Poisons Tolerance. *Catalysts*, 10 (6), 594. DOI: 10.3390/catal10060594.
- [25] Bauer, F., Ficht, K., Bertmer, M., Einicke, W.-D., Kuchling, T., Gläser, R. (2014). Hydroisomerization of long-chain paraffins over nano-sized bimetallic Pt–Pd/H-beta catalysts. *Catalysis Science & Technology*, 4 (11), 4045–4054. DOI: 10.1039/C4CY00561A.
- [26] Bi, Y., Xia, G., Huang, W., Nie, H. (2015). Hydroisomerization of long chain n-paraffins: the role of the acidity of the zeolite. *RSC Advances*, 5 (120), 99201–99206. DOI: 10.1039/C5RA13784E.